Electric Equivalent Circuit of a NiMH Cell: Methods and Results

E. Kuhn, Phd Student, Université de Technologie de Compiègne
Laboratoire d'Electromécanique de Compiègne (LEC)
BP20529 60205 COMPIEGNE Cedex
Fax :03.44.20.48.13, emmanuel.kuhn@utc.fr

C. Forgez, Assistant Professor, Université de Technologie de Compiègne
Laboratoire d'Electromécanique de Compiègne (LEC)
BP20529 60205 COMPIEGNE Cedex
Fax :03.44.20.48.13, christophe.forgez@utc.fr

G. Friedrich, University Professor, Université de Technologie de Compiègne
Laboratoire d'Electromécanique de Compiègne (LEC)
BP20529 60205 COMPIEGNE Cedex
Fax :03.44.20.48.13, guy.friedrich@utc.fr

Abstract

We already have presented at EVS 17 [1] optimal control strategies for an hybrid parallel vehicle. Compared to usual strategies, the control laws we defined for the electrical and thermal engines are independent of any driving cycle. These works in a first step did not take into account the battery efficiency.
According to refine our control laws, we started in 2001 a three years study on modeling a 42V 13.5Ah NiMH battery pack made of thirty two commercially available 1.2V 13.5Ah cells. This 42V structure has been chosen to anticipate the future voltage standards in automotive. We present and justify in this paper two models: a dynamic one using non integer derivatives that gives the voltage response of the pack when submitted to any current profile, and an energetic one that gives Joule losses during energetic transfers.
Both models use an equivalent electric scheme, whose components are identified by an experimental technique called "Electrochemical Impedance Spectroscopy (E.I.S)".

Keywords: Dynamic model, Energetic efficiency, Batteries, NiMH, Spectroscopy

Introduction

Assuming a battery efficiency of 100%, the control laws we have presented in EVS 17 [1] gave us the electric energy that could be removed or restored during acceleration and deceleration phases.
This strategy has been established for any kind of hybrid vehicle and for any driving cycle.
Since control laws applied to the electrical engine depend on the energetic efficiency of the battery, an accurate knowledge of its energetic behaviour is necessary.
Hence two models have been developped .
The first one is dedicated to dynamic applications, and is used to calculate the voltage responses of the battery when submitted to any current profile.
The second one is dedicated to energetic applications, and is used for instantaneous power and energy calculations. It can possibly be used for dynamic calculations.
Both models are based on lumped constant equivalent electric circuits, which are identified from "Electrochemical Impedance Spectroscopy".

The following sections deal with:

- Justification and validation of the dynamic model
- Justification and validation of the energetic model

1. State of the art in battery modeling

1.1 State of the art in dynamic modeling

Two methods are encountered in battery modeling.
On one hand, electrochemical phenomena are described in the form of differential equations and then solved [2]. Such an approach needs the knowledge of the initial and boundary conditions of the cell, which are not always available.
On the other hand, an equivalent electrical circuit is proposed, whose components are identified by experimental measures [3]. Transmission lines, electrical networks or resistive companion models come from this approach [4][5].
Although this method has been widely used to model lead-acid batteries, it has been rarely applied to NiMH cells. Our study tries to fill this lack by presenting a dynamical model of a 13.5Ah 42V NiMH battery.

1.2 State of the art in energetic modeling

Two methods can be used to figure out the energetic efficiency of a battery during charge or discharge operations.
On one hand by estimating heat flows, we can get Joule losses and then characterize the process efficiency. Such a method calls for the knowledge of temperature and entropy variations [6].

On the other hand, when the battery is represented by an equivalent electric scheme [7] [8], the dissipated and stored energy during energetic transfers can be immediately calculated since it is related to resistive and capacitive elements. This is the way we have chosen to estimate the Joule losses of our 42V 13.5Ah NiMH pack.

2. Dynamic model of the 13.5Ah 42V NiMH pack

Since the 42V pack used in our electrical powertrain bench is made of thirty two 1.2V 13.5Ah elements in series, we first modeled a single cell, and then deduced the equivalent model for the entire pack.
These issues are respectively tackled in the coming sections.

2.1 Dynamic model of a single 1.2V 13.5Ah element

We consider for a single NiMH element the equivalent electric circuit of Figure 1.

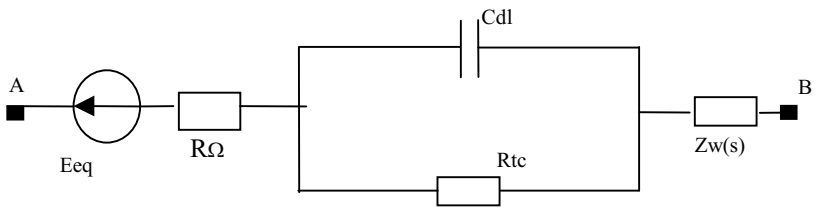

Figure 1: Equivalent electric scheme of a single 1.2V 13.5Ah NiMH cell

This scheme has been obtained from the works of Notten and Randles [9][10]; its complete justification can be found in [11].
Looking at Figure 1, we find the following electrical elements representing either a static or a dynamic electrochemical phenomenon:

- E_{eq} stands for the equilibrium potential of the cell.
- R_{tc} and C_{dl} stand for charge transfer phenomena occuring in high frequencies.
- Z_w represents the diffusion phenomena occuring in low frequencies. This equivalent impedance is called "Warburg impedance"[9], its structure is detailed in the coming section.

2.2 Structure of the warburg impedance Z_w.

According to find the structure of Z_w, (which usually depends on the type and the boundary conditions of the considered cell), we performed on our single element at several state of charges (SoC) spectroscopy measurements.

We briefly remind the principle of this technique commonly used when characterizing any electrochemical system [12].

A low sinus voltage v(t)=Vmax sin(ωt) of given frequency and given amplitude (Vmax below 10mV) is superimposed to the equilibrium voltage of the cell at a given state of charge.

The corresponding sinus current i(t)=Imaxsin(ωt + φ) flowing through the battery is then measured.

When dividing the sinus voltage by the sinus current we obtain the impedance cell $Z_T(s)$ such as : $Z_T(s)=\frac{V_{\max}}{I_{\max}}\exp(j\varphi)$,where φ is the phase shift between v(t) and i(t).

At a given state of charge when sweeping the frequency from 0.001Hz to 46Hz we obtain the "Impedance spectrum" of the cell.

From the collected data, we displayed the bode plots of $Z_T(s)$ ie: GdB (ω)=20.log $|Z_T(s)|$ Figure 2.

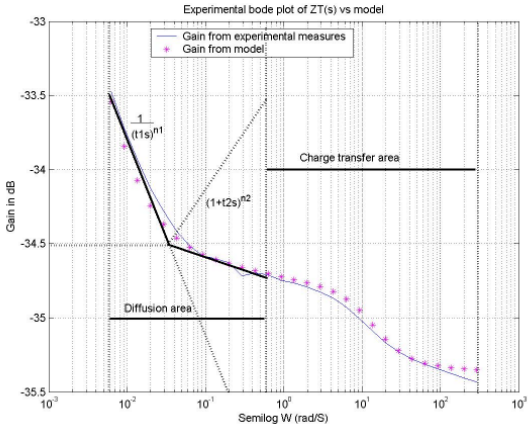

Figure 2 : Bode plot of $Z_T(s)$ at SoC 80%(experimental versus model)

As can be seen in Figure 2 in low frequencies, the gain of $Z_T(s)$ can be reached by two asymptotes. One of these is a non integer integrator $H_1(s)=\frac{1}{(\tau_1 s)^{n_1}}$, the other one is a high pass function $H_2(s)=(1+\tau_2 s)^{n_2}$.

At least the expression of Zw(s) is easily deduced from the combination of these non integer functions.

$$Z_W(s)=H_1(s).H_2(s)=\frac{(1+\tau_2 s)^{n_2}}{(\tau_1 s)^{n_1}} \quad (1)$$

As can be seen in equation (1), the transfer function used to represent $Z_w(s)$ is made of non integer power of the Laplace variable s, which in time domain corresponds to non integer derivatives [13].

2.3 Parameters identification

From the equivalent electric model defined in Figure 1, and the structure of $Z_w(s)$ given by equation (1), the expression of the cell impedance $Z_T(s)$ is such as:

$$Z_T(s) = R_\Omega + \frac{R_{tc}}{1 + s.R_{tc}C_{dl}} + \frac{(1+\tau_2 s)^{n_2}}{(\tau_1 s)^{n_1}} \tag{2}$$

Assuming N data have been collected from Spectroscopy, R_{tc}, C_{dl}, n_1, n_2, τ_1, τ_2 are identified through the minimization of the following criteria Cr (equation (3)).

$$Cr = \sum_{k=1}^{N} [\mathrm{Im}(Z_{Tactual}(j\omega_k) - \mathrm{Im}(Z_T(j\omega_k))]^2 + [\mathrm{Re}(Z_{Tactual}(j\omega_k) - \mathrm{Re}(Z_T(j\omega_k))]^2 \tag{3}$$

Due to the parasitic resistances of the spectroscopy bench, R_Ω has not been included in the minimizing criteria Cr. We found it in continuous regime, applying at different state of charges several current pulses $\Delta i(t)$.The corresponding voltage drop $\Delta v(t)$ was then recorded and R_Ω got from the ratio:

$$\frac{\Delta v(t)}{\Delta i(t)} = R_\Omega \tag{4}$$

2.4 Frequential validation of the model

According to check the accuracy of our model, we compared the nyquist plots obtained from spectroscopy measurements to those rebuilt from the model. Figure 3.

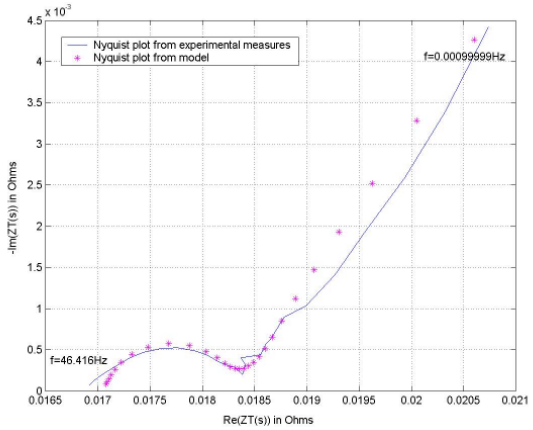

Figure 3 : Comparison of the nyquist plots at SoC 80%.(Experimental measures and model).

As can be seen on Figure 3, our model fits well experimental data.

2.5 Model validation in time domain

The validity of our model has been checked in time domain, by applying to our single 1.2V 13.5Ah cell several current profiles at different state of charges.
The voltage responses of the model calculated with equation (5) was then compared to the experimental ones.

$$v_{\mathrm{mod}\,el}(t) = E_{eq} + R_\Omega i(t) + L^{-1}\left(\frac{R_{tc}I(s)}{1 + sR_{tc}C_{dl}}\right) + L^{-1}\left(\frac{(1+\tau_2 s)^{n_2} I(s)}{(\tau_1 s)^{n_1}}\right) \tag{5}$$

Where L^{-1} stands for the inverse Laplace transform

For all these simulations (Figure 4) the maximum errors in percent have been calculated and are presented in Table 1. We remind the definition we used for error estimation in equation (6).

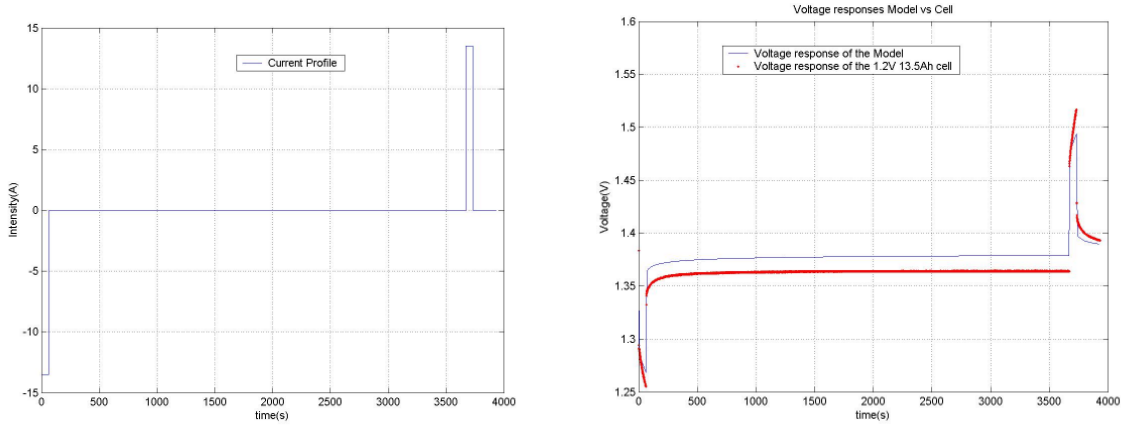

Figure 4 :Current profile set to a 1.2V 13.5Ah cell with its corresponding voltage responses. Simulation performed at a state of charge of 80% , **|Imax|=13.5A.**

$$\varepsilon(t) = 100.\frac{\left|v_{actual}(t) - v_{\mathrm{mod}el}(t)\right|}{v_{actual}(t)} \qquad (6)$$

Table 1: Maximum errors for different curent profiles and amplitudes at SoC 100% and SoC 80%

SoC 100%	**|Imax|=2.7A**	**|Imax|=6.75A**	**|Imax|=13.5A**	**|Imax|=27A**	**|Imax|=67.5A**
Max(ε(t))	0.6%	1%	1.2%	1.8%	(*)
SoC 80%	**|Imax|=2.7A**	**|Imax|=6.75A**	**|Imax|=13.5A**	**|Imax|=27A**	**|Imax|=67.5A**
Max(ε(t))	0.7%	1%	1.8%	3%	(*)

(*) Since an applied current such as |Imax|=5C=67.5A is damaging for the cell, we kept our simulations to |Imax|=2C=27A

2.6 Dynamic model of the 42V 13.5Ah pack

Since our 42V NiMH pack is made of thirty two 1.2V elements in series, its equivalent circuit is that of Figure 5.

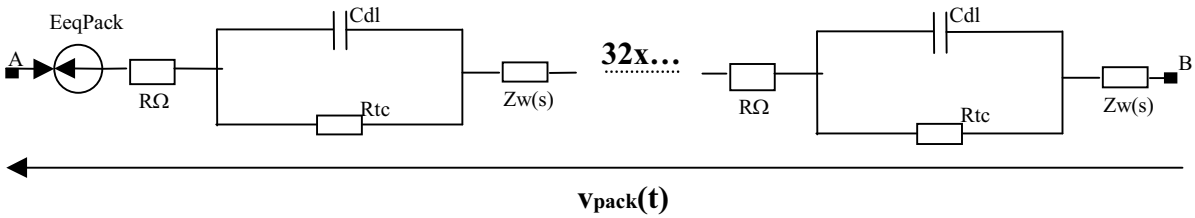

Figure 5 : Model of the 42V 13.5Ah pack

The voltage response of the pack when submited to a given current i(t) is such as:

$$v_{Pack}(t) = E_{eqPack} + 32 * \left[R_{\Omega} i(t) + L^{-1}\left(\frac{R_{tc} I(s)}{1 + sR_{tc}C_{dl}} \right) + L^{-1}\left(\frac{(1+\tau_2 s)^{n2}\, I(s)}{(\tau_1 s)^{n1}} \right) \right]$$

Since the state of charge of a battery in a mild hybrid application remains between 60% and 95%, we checked our model by applying to the pack three different current profiles at SoCs 60%, 80%, and 95%. Figures 6, 7, 8 are typical examples of the simulations we performed at a state of charge of 80%.

Because of the limitations of the electrical devices we used in this validation, current amplitude never exceeded +/-4A.

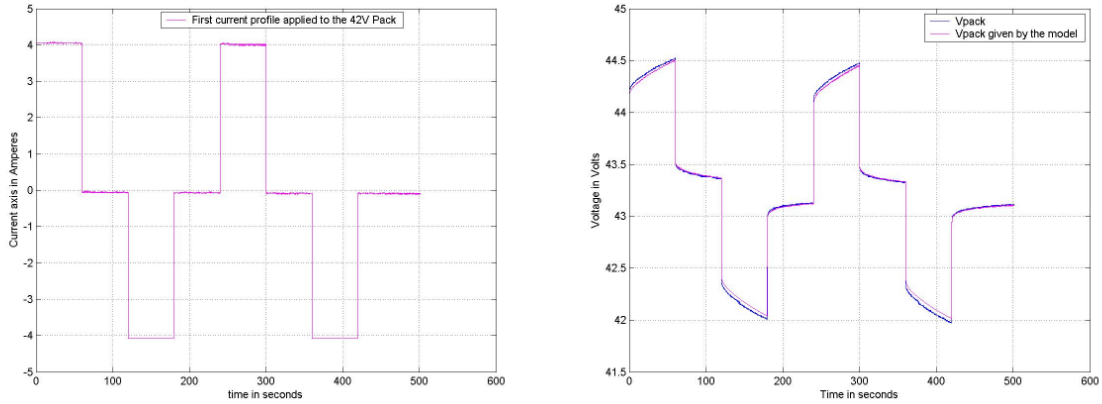

Figure 6 : Current profile (a) with the associated voltage responses at a SoC of 80%.

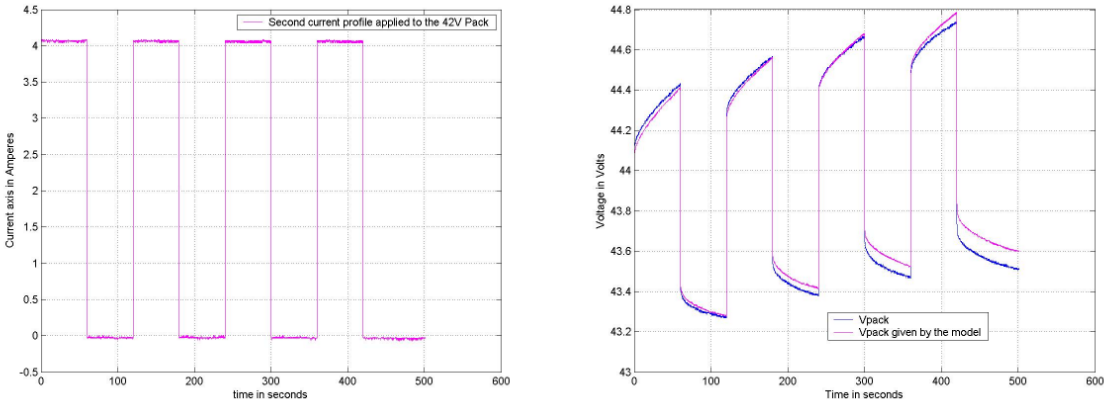

Figure 7 : Current profile (b) with the associated voltage responses at a SoC of 80%.

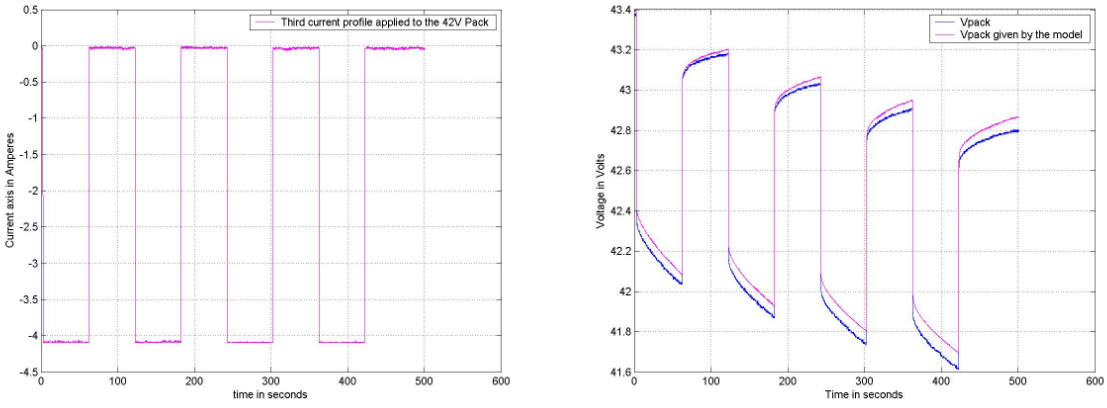

Figure 8 : Current profile (c) with the associated voltage responses at a SoC of 80%.

The maximum errors between the voltage responses of the pack and the model have been calculated according to the criteria of equation (7) and are presented in Table 2.

$$\varepsilon(t) = 100.\frac{\left|v_{actual}(t) - v_{Pack}(t)\right|}{v_{actual}(t)} \qquad (7)$$

Table 2: Comparison between voltage responses of the pack and the model for specific current profiles.

42V Pack	Current profile (a)	Current profile (b)	Current profile (c)
SoC 60% Max(ε(t))	0.35%	0.4%	0.9%
SoC 80% Max(ε(t))	0.2%	0.17%	0.48%
SoC 95% Max(ε(t))	0.6%	0.7%	1%

As can be seen in Table 2, errors remains satisfactory and confirm the good results we already obtained for a single element.

3. Energetic model of the 13.5Ah 42V NiMH pack

3.1 Energetic model of a single 1.2V 13.5Ah cell

Power and energy losses during energetic transfers can be obtained by calculating entropy variations. Such an approach calls for the knowledge of many experimental parameters which are not always available.
An easier way to determine Joule losses is to represent the studied cell by an equivalent circuit only made of resistive and capacitive elements.
This is the way we chose to assess the losses of our 42V pack.
The structure made of non integer derivatives we chose for the Warburg impedance does not allow us to identify dissipative or capacitive elements, it is not convenient for energetic calculations.
Hence a new structure only made of resistive and capacitive elements must be defined for $Z_w(s)$.
Such structures have already been applied when modeling lead-acid batteries or supercapacitors [14].
We retrieved a structure already used to model lead-acid battery diffusion, and applied it on the NiMH pack [15].
The new transfer function $Z_w'(s)$ we use to model diffusion phenomena is given by equation (8)

$$Z_{w'}(s) = \frac{k_2}{\sqrt{s}} \tanh\left(\frac{k_1}{k_2}\sqrt{s}\right) \tag{8}$$

On the opposite to the transfer function we used for $Z_w(s)$, $Z_w'(s)$ has a physical interpretation of diffusive phenomena.
To figure out the equivalent lumped constant electric scheme corresponding to $Z_w'(s)$, we first calculate its inverse Laplace tranform $Z_w'(t)$. The result is given by equation (9) and justified in [15].

$$Z_{w'}(t) = L^{-1}(Z_w'(s)) = L^{-1}\left(\frac{k_2}{\sqrt{s}}\tanh\left(\frac{k_1}{k_2}\sqrt{s}\right)\right) = \frac{2k_2^2}{k_1}\sum_{n=1}^{\infty}\exp\left(-\frac{(2n-1)^2\pi^2 k_2^2}{4k_1^2}t\right) \tag{9}$$

Then we develop equation (9) to get equation (10)

$$Z_{w'}(t) = \frac{2k_2^2}{k_1}.\exp\left(-\frac{\pi^2 k_2^2}{4k_1^2}t\right) + \frac{2k_2^2}{k_1}.\exp\left(-\frac{(3)^2\pi^2 k_2^2}{4k_1^2}t\right) + \ldots + \frac{2k_2^2}{k_1}.\exp\left(-\frac{(2n-1)^2\pi^2 k_2^2}{4k_1^2}t\right) \tag{10}$$

Actually equation (10) can be rewritten as

$$Z_{w'}(t) = \frac{1}{C}.\exp\left(-\frac{t}{R_1 C}\right) + \frac{1}{C}.\exp\left(-\frac{t}{R_2 C}\right) + \ldots + \frac{1}{C}.\exp\left(-\frac{t}{R_n C}\right) \tag{11}$$

By comparing equation (11) and equation (10) we can deduce the expressions of R_n and C.

$C = \frac{k_1}{2k_2^2}, R_n = \frac{8k_1}{(2n-1)^2\pi^2}$ with k_1 and k_2 identified from Spectroscopy.

If we calculate the Laplace transform of equation (11) we get the following expression (equation(12)).

$$Z_{w'}(s) = \frac{1}{C}.\frac{1}{s+\frac{1}{R_1C}} + \frac{1}{C}.\frac{1}{s+\frac{1}{R_2C}} + \ldots \frac{1}{C}.\frac{1}{s+\frac{1}{R_nC}} \quad (12)$$

equation (12) clearly shows that Z_w'(s) corresponds to an infinite sum of RC circuits. The equivalent electric circuit of Z_w'(s) is shown Figure 9.

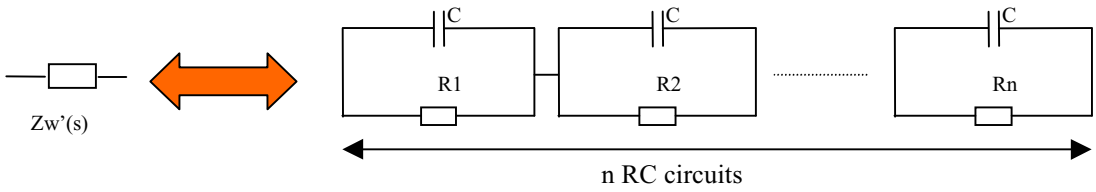

Figure 9 : Warburg impedance under the form of n RC networks

If we add to this electric circuit the equilibrium potential E_{eq}, the internal resistance R_Ω and the R_{tc} C_{dl} network related to charge transfer phenomena, we get the energetic model of a single 1.2V 13.5Ah NiMH element in time domain (Figure 10).

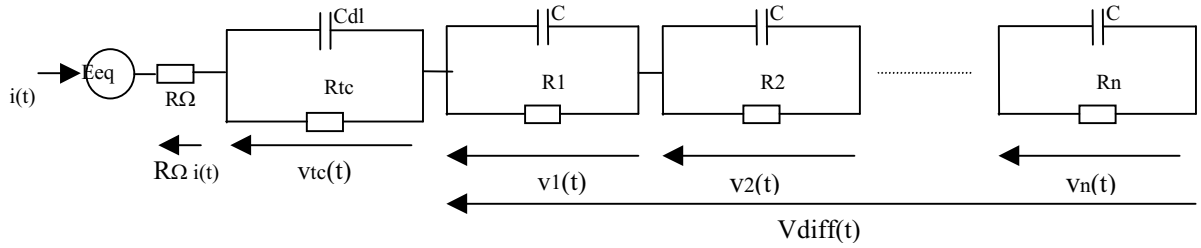

Figure 10 : Energetic model of a single 1.2V 13.5Ah NiMH cell

3.2 Frequential validation of the energetic model

According to evaluate the accuracy of this new model we superimposed the Nyquist plots obtained from spectroscopy to those rebuilt with Z_T'(s) given by equation (13). Figure 11.

$$Z_T'(s) = R_\Omega + \frac{R_{tc}}{1+s.R_{tc}C_{dl}} + \frac{k_2}{\sqrt{s}}\tanh\left(\frac{k_1}{k_2}\sqrt{s}\right) \quad (13)$$

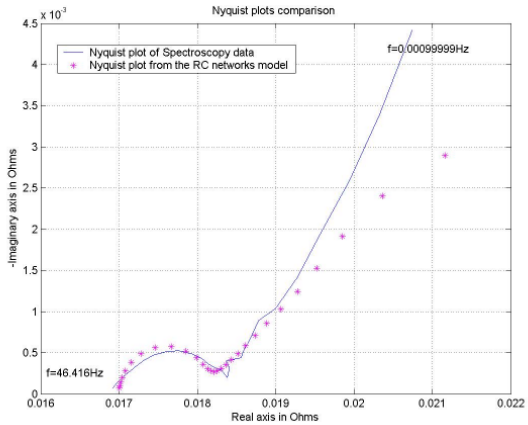

Figure 11: Comparison of the nyquist plots at SoC 80%.(Experimental measures and model).

As it can be seen in Figure 11, the transfer function $Z_T'(s)$ using RC networks shifts from experimental data in low frequencies. Complementary works have proved that this lack of accuracy in low frequencies had few consequences in time domain. Actually we could also use this new structure based on RC networks instead of the previous model in dynamic applications.

3.3 Joule losses calculations for a single element and the entire pack

In practical calculations we can not take an infinite number of RC circuits. Hence a compromise must be found between the accuracy of our results and the time it will take to get them (fifteen RC circuits seems to be the right trade off).
The Joule losses of a single element are given by equation (14)

$$pj(t) = R_\Omega .i(t)^2 + \frac{v_{tc}(t)^2}{R_{tc}} + \sum_{n=1}^{15} \frac{v_n(t)^2}{R_n} \tag{14}$$

Since the 42V pack is made of thirty two elements in series, its Joule losses are given by equation (15).

$$pj_{Pack}(t) = 32.[R_\Omega .i(t)^2 + \frac{v_{tc}(t)^2}{R_{tc}} + \sum_{n=1}^{15} \frac{v_n(t)^2}{R_n}] \tag{15}$$

3.4 Validation of the Energetic model

According to check the validity of the energetic model, we applied to our 42Vpack two symetric current profiles at SoC 60%, SoC 80%, and SoC 95%. Figure 12

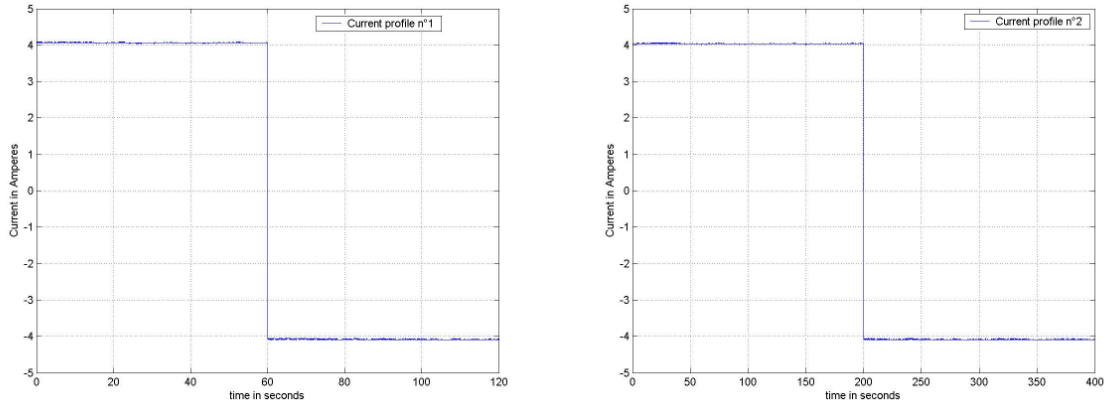

Current profile (a) Current profile(b)

Figure 12: Current profiles used for energetic validation .

For both of these currents we superimposed the instantaneous power of the battery $p_{batt}(t)$ to $p_{model}(t)$ given by equation (16). Fifteen RC networks have been taken for calculations.

$$p_{model}(t) = \left(E_{eqPack} + 32.[R_\Omega .i(t) + v_{tc}(t) + \sum_{n=1}^{15} v_n(t)]\right) i(t) \tag{16}$$

During these energetic transfers we also have compared the energy flowing in and out of the battery $e_{batt}(t)$ to $e_{model}(t)$ given by equation (17). Again 15 RC networks have been taken for numeric calculations.

$$e_{model}(t) = \int_{t=0}^{t} p_{model}(t).dt \tag{17}$$

Figures(12) represents the results we got at SoC 80% for current profile (a).

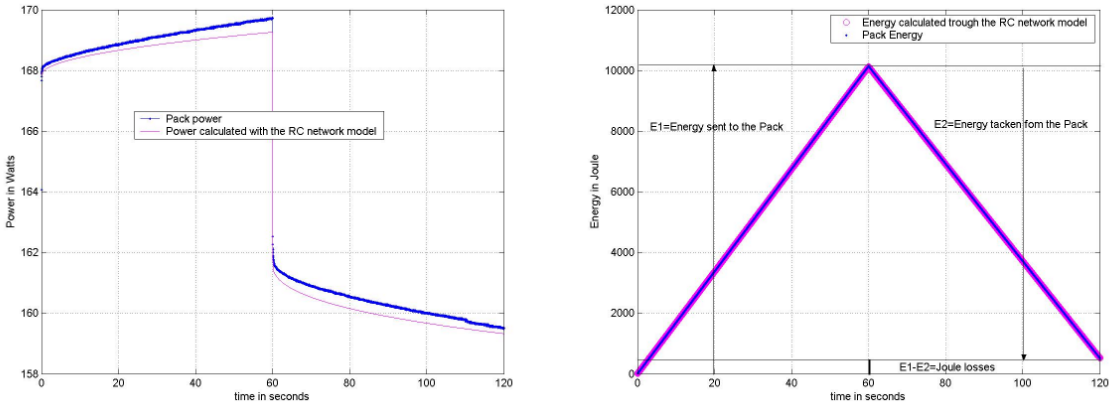

Figure 12 : Power and Energy comparisons at SoC 80% for curent profile (a)

Errors between instantaneous powers and energies have then been reported in Table 3 with the following definitions of εpower(t) and εenergy(t) (equation (18)).

$$\varepsilon_{energy}(t) = 100.\left|\frac{e_{pack}(t) - e_{\mathrm{mod}el}(t)}{e_{Pack}(t)}\right|, \varepsilon_{power}(t) = 100.\left|\frac{p_{pack}(t) - p_{\mathrm{mod}el}(t)}{p_{Pack}(t)}\right| \quad (18)$$

Table 3: Errors between instantaneous powers and energies

SoC 60%	**Current profile (a) 0<t<120s**	**Current profile (b) 0<t<400s**
Max(εpower(t))	0.6%	1.28%
Max(εenergy(t))	1.9%	3.32%
SoC 80%	**Current profile (a) 0<t<120s**	**Current profile (b) 0<t<400s**
Max(εpower(t))	0.27%	0.8%
Max(εenergy(t))	0.78%	2.1%
SoC 95%	**Current profile (a) 0<t<120s**	**Current profile (b) 0<t<400s**
Max(εpower(t))	0.26%	0.55%
Max(εenergy(t))	2.77%	0.97%

Conclusion

Impedance Spectroscopy is a powerful tool when characterizing battery dynamics.
With this method we defined two lumped constants battery models, whose reliability has been checked on several current profiles.
The first one based on non integer derivatives is dedicated to dynamic applications and turns out to be a good representation of diffusion phenomena.
The other one is dedicated to energetic calculations, in order to define battery efficiency during charge and discharge operations.
With this model we will refine the control laws presented in EVS 17, and assess the real amount of energy stored in the battery during decceleration phases and available energy from the battery during acceleration phases.
Once we have improved our control laws we will check them on an powertrain bench whose electrical features are those of a mild hybrid vehicle: a 42V NiMH battery pack associated to a 7kW DC engine.
Those results will be presented in the next EVS meeting.

References

[1] C.Forgez, G.Friedrich, J.M.Biedinger, *Method to find the hybridization rate for a parallel hybrid electrical vehicle*, EVS 17,October 2000.

[2] E.Karden, P.Mauracher, *Electrochemical modeling of lead/acid batteries under operating conditions of electric vehicles*, Journal of power sources 64:175-180,1997.

[3] M.Ceraolo, *New dynamical models of lead-acid batteries*, IEEE transactions on power systems, 15(4):1184-1190, November 2000.

[4] T.Brumleve, *Transmission line equivalent circuit models for electrochemical impedances*, Journal of Electroanalytical Chemistry, 126:73-104, 1981.

[5] J.Horno and M.T.Garcia-Herrnandez, *Digital simulation of electrochemical process by the network approach,* Journal of Electroanalytical Chemistry, 352:83-97, 1993.

[6] P.H.L Notten, W.S.Kruijt and H.J.Bergveld, *Electronic network modeling of rechargeable batteries :Part II The NiCd system*, 191st Electrochemical Society Meeting Montreal, May 1997.

[7] Jincan Chen, Yinghui Zhou, *Minimum Joule heating dissipated in the charging process of a rechargeable battery*, Energy 26:607-617, 2001.

[8] A. Bejan, N.Dan, *Maximum work from an electric battery model*, Energy 22:93-102,1997.

[9] P.H.L Notten, *Electronic-network modeling of rechargeable NiCd cells and its application to the design of battery management systems*, Journal of power sources 77:143-158, 2000.

[10] A Bard, *Electrochemical methods Fundamentals and applications*, J Wiley and sons, 2nd edition, 2000.

[11] E.Kuhn, *Modèle de Batterie NiMH pour véhicule hybride parallèle: validation en grands signaux*, J.C.G.E, Saint-Nazaire, June 2003.

[12] F.Huet, *A review of impedance measurements for determination of the state of charge or state of health of secondary batteries*, Journal of power sources 87:12-20,2000.

[13] A.Oustaloup, *La dérivation non entière*, Hermès,1995.

[14] S.Buller, E.Karden, *Modeling the dynamic behavior of Supercapacitors using Impedance Spectroscopy*, IEEE Transaction on Industry Applications vol 38 n°6,1622:1626, November 2002.

[15] P.Mauracher, E.Karden, *Dynamic modeling of lead/acid batteries using impedance spectroscopy for parameter identification*, Journal of power sources 67:69-84,1997.